Biomedicine & Pharmacotherapy 167 (2023) 115449

Contents lists available at ScienceDirect

Biomedicine & Pharmacotherapy

journal homepage: www.elsevier.com/locate/biopha

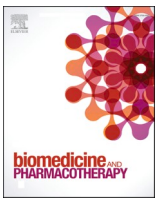

# Therapeutic potential of mesenchymal stem cell-derived exosomal miR-296-5p and miR-337-3p in age-related erectile dysfunction via regulating PTEN/PI3K/AKT pathway

Kefan Li [a], Ruiyu Li [a], Zongyong Zhao [c], Chen Feng [a], Shuai Liu [a,b,d,*], Qiang Fu [a,b,d,*]

[a] Department of Urology, Shandong Provincial Hospital, Shandong University, Jinan, China
[b] Department of Urology, Shandong Provincial Hospital Affiliated to Shandong First Medical University, Jinan, China
[c] Department of Urology, Liaocheng Third People's Hospital, Liaocheng, Shandong, China
[d] Engineering Laboratory of Urinary Organ and Functional Reconstruction of Shandong Province, Shandong Provincial Hospital affiliated to Shandong First Medical University, Jinan, China

ARTICLE INFO

*Keywords:*
Age-related erectile dysfunction
Mesenchymal stem cells
Exosomes
MiRNA
Corpus cavernosum smooth muscle cells
PTEN/PI3K/AKT pathway

ABSTRACT

Mesenchymal stem cells (MSCs) are viewed as an increasingly promising treatment for age-related erectile dysfunction (AED). Owing to the limitations of injecting living cells, the injection of exosomes appears to be a more plausible option. However, whether MSC-derived exosomes (MSC-Exos) improve AED and their potential mechanism remains unknown. MSC-Exos were prepared and injected intracavernously into aged rats to determine their effects on AED. Masson's trichrome staining was used to ascertain the changes in the histological structure of the corpus cavernosum. Then miRNA sequencing of MSC-Exos and analysis of the critical exosomal miRNAs were performed, as well as their target pathway enrichment analysis. Real-time quantitative PCR (RT-qPCR) and Western blot assay were performed to reveal the functions of MSC-Exos in regulating the PTEN/PI3K/AKT signaling pathway. Moreover, the effects of MSC-Exos on the corpus cavernosum smooth muscle cells (CCSMCs) apoptosis are explored in vitro. The experimental data validate that intracavernous injection of MSC-Exos ameliorated erectile function in AED rats. Masson's trichrome staining shows MSC-Exos therapy restores the histological structure of the corpus cavernosum by improving the ratios of smooth muscle to collagen. The exosomal miR-296–5p and miR-337–3p target and inhibit PTEN, modulating the PI3K/AKT signaling pathway. Furthermore, exosomes inhibit the apoptosis of CCSMCs. Our findings suggest that MSC-Exos improve AED by delivering miR-296–5p and miR-337–3p to regulate the PTEN/PI3K/AKT signaling pathway. These results bode well for the therapeutic potential of MSC-Exos for AED treatment.

## 1. Introduction

Erectile dysfunction (ED) is projected to impact 322 million people by 2025, making it a severe health concern for an increasingly healthy aging population [1]. According to epidemiologic research, aging is an independent risk factor for ED, regardless of concomitant conditions such as diabetes mellitus and cardiovascular diseases [2]. With age, the prevalence and severity of ED rise steadily [3,4]. However, essential mechanisms involved in age-related erectile dysfunction (AED) remain incompletely understood. The possible causes of AED include impaired nitric oxide synthase (NOS) generation and redundant oxidative stress (OS) levels, which are driven mainly by endothelial dysfunction [5]. Phosphodiesterase type 5 inhibitors (PDE5i), such as sildenafil and tadalafil, are commonly used to treat ED in men of various ages and aetiologies [6]. However, they show low responsiveness and adverse effects such as flushing, dyspepsia, and headaches [7,8]. Therefore, expanding more effective and feasible protocols for AED is urgently required.

The application of mesenchymal stem cells (MSCs) in regenerative medicine is a promising research topic with the potential to differentiate into a broad spectrum of cell types under specific circumstances. Recently, therapies around MSCs have been proven to have therapeutic implications in AED treatment [9,10]. Bone marrow-derived mesenchymal stem cells (BMSCs), a sort of MSC, have been demonstrated to

* Correspondence to: Department of Urology, Shandong Provincial Hospital Affiliated to Shandong First Medical University, 9677 JingshiRoad, Jinan, Shandong Province 250021, China.
*E-mail addresses:* liushuai@sdfmu.edu.cn (S. Liu), qiangfu68@163.com (Q. Fu).

https://doi.org/10.1016/j.biopha.2023.115449
Received 10 July 2023; Received in revised form 1 September 2023; Accepted 4 September 2023
Available online 8 September 2023

bring numerous benefits over other stem cells, including being readily *ex vivo* expanded, the convenience of isolating, rapid proliferation speed, security and safety, and minimal immunogenicity [11]. MSCs have been identified as potentially improving AED by secreting growth factors and cytokines to repair injured penile tissues [12]. Notably, along with releasing soluble substances, MSCs can also secrete extracellular vesicles (EVs) as vehicles for delivering modulatory proteins, nucleic acids, and lipids to stimulate the activation of tissue-resident receptor cells [13,14].

As a class of EVs, exosomes receive increased attention and have been established as physiologically significant components of the MSC secretome [15]. Exosomes refer to endosomal membrane vesicles with 40–150 nm diameters derived from multivesicular endosomes or multivesicular bodies [16]. They contain many complex molecules, such as proteins, mRNAs, and microRNAs (miRNAs), which can modulate intracellular signal transduction pathways [17]. MSC-derived exosomes (MSC-Exos) are considered therapeutic agents to curtail tissue damage and promote healing in several diseases, including age-related complications [18]. The application of MSC-Exos has been revealed to improve ED induced by diabetes mellitus or cavernous nerve injury [19,20]. It has been found that MSC-Exos can release miRNAs, which play a pivotal role in restoring diabetic ED [21]. In addition, compared with stem cell implantation therapy, the injection of exosomes shows a low propensity for triggering immunological responses, lowering the risk of heterotopic implantation. However, reports on MSC-Exos therapy for AED are relatively rare.

MiRNAs are tiny non-coding RNAs with 17–24 nucleotides that bind to the 3′-untranslated region or open reading frame of target mRNAs for cleavage or translational repression [22]. MiRNAs have been revealed to influence a range of cellular processes, including proliferation, apoptosis, and senescence [22,23]. Also, AED was found to be linked to a collection of genes related to aging that are controlled by different miRNAs [24].

In this study, we utilized exosomes derived from MSCs as the therapeutic medium and investigated the effect of MSC-Exos on improving erectile function in AED rats. Moreover, miRNA sequencing was conducted in MSC-Exos and MSCs to further elucidate the probable mechanism behind MSC-Exos therapy. The role of critical exosomal miRNAs in the PTEN/PI3K/AKT signaling pathway was also investigated. The effect of MSC-Exos on corpus cavernosum smooth muscle cells (CCSMCs) apoptosis was also explored in vitro. Our findings confirm the application of MSC-Exos in alleviating AED for the first time, indicating that this might represent a novel therapeutic approach for treating AED.

## 2. Materials and methods

### 2.1. MSC-Exos isolation and identification

The bone marrow mesenchymal stem cells of the Sprague Dawley rat were acquired from the Chinese Academy of Sciences Cell Bank. MSCs were grown in Mesenchymal Stem Cell Medium (ScienCell Research Laboratories) supplemented with mesenchymal stem cell growth supplement (MSCGS), 10% fetal bovine serum (FBS) (Gibco, USA), and 1% penicillin/streptomycin (Gibco, USA) at 37 °C and 5% $CO_2$. At 80% confluence, MSCs were rinsed twice in phosphate-buffered solution (PBS) and then incubated for 48 h in a serum-free stem cell medium (Gibco, USA). The supernatant was obtained and centrifuged for 30 min at 4 °C and 2000 g to remove dead cells and cellular debris. The supernatant was filtered through an aseptic membrane (Millipore, Billerica, MA, USA) and ultracentrifuged overnight at 4 °C and 120,000g. The precipitate was resuspended in cold PBS and ultracentrifuged for 2 h at 4 °C and 120,000g. For immediate or future analyses, the granules of isolated exosomes were resuspended in 200 μl of cold PBS and stored at − 80 °C. Afterwards, transmission electron microscopy (TEM) was used to characterize the morphology of isolated MSC-Exos. The quantification of exosomes was determined by the protein concentration using an BCA quantification reagent (P0010S, Beyotime, Shanghai, China) according to previous literature [25]. A western blot assay identified the specific MSC-Exos markers CD63 and tumor susceptibility gene 101 (TSG101). Using a Zetaview instrument (PMX110, Particle Metrix, München, Germany), nanoparticle tracking analysis (NTA) was conducted to determine the size of MSC-Exos.

### 2.2. Lentivirus construction, package, and transfection

Lentiviruses were used to carry out the overexpression of the miR-296–5p or miR-337–3p. The lentiviral constructs were packaged using a second-generation packaging system. Transfection was performed on cells at a confluence of 70%−80%. Briefly, the 293 T cells were co-transfected with the recombinant GV369 plasmid expressing miR-296–5p or miR-337–3p, pHelper 1.0 and pHelper 2.0 in serum-free medium at 37 ℃ and 5% CO2 for 6 h. Then, discard the medium containing the transfection mixture, add 20 ml medium containing 10% serum, and continue culturing for 48 h in a 37 °C, 5% $CO_2$ incubator. The cell suspension was centrifuged at 4000g for 10 min. Lentivirus-rich supernatants were collected and filtered using a 0.45 μm syringe filter. Lentivirus was stored at −80 °C before being injected into the corpus cavernosum of AED rats.

### 2.3. Animal experiments

The 24-month-old (aged) and 10-week-old (normal) male Sprague-Dawley (SD) rats were obtained from the Laboratory Animal Center of Shandong University (Jinan, China). The Animal Care and Use Committee of Shandong University authorized all animal treatment experimental procedures (NO.2022–0024, Jinan, China). All animals were confined in a pathogen-free (SPF) environment at 22–24 °C with a weekly 12-h light–12-h dark cycle and access to food and water. After apomorphine (100 μg/kg) assay selection, 48 AED rats (24 months) were randomly divided into six treatment groups (n = 8 per group): PBS, MSC, Exos 50 μg, Exos 100 μg, MSC + Exos inhibitor (GW4869, D1692, 10 μM, Sigma-Aldrich), and Exos 100 μg + AKT1/2 kinase inhibitor (0.5 μmol, Sigma). The eight 10-week-old male SD rats are considered the normal control group (NC). All treatments were administered by intracavernous injection. The administration volume in all treatment groups was diluted to 100 μl with PBS. Moreover, to identify the role of miR-296–5p and miR-337–3p in vivo, the lentiviruses loaded with miR-296–5p or miR-337–3p ($1 \times 10^9$ TU/ml, 20 μl) were injected into the corpus cavernosum of AED rats for the transfection groups (n = 8). In contrast, empty vectors were injected into AED rats for the control AED group (n = 8).

### 2.4. Assessment of erectile function

Four weeks after injection, maximal intracavernous pressure (max ICP) and mean systemic artery pressure (MAP) were measured in each rat. The max ICP/MAP ratios were utilized to evaluate erectile function. The rats were face-up after intraperitoneal anaesthesia with avertin (280 mg/kg). The left carotid artery was then cannulated with a PE-50 catheter (Becton Dickinson & Co., Sparks, MD) to monitor systemic arterial blood pressure. The ICP was measured by inserting a 23-gauge catheter containing 250 U/ml of heparinized saline into the corpus cavernosum. After locating the pelvic ganglia and isolating the cavernous nerve, we stimulated it for 60 s with an electrode (5 ms; 15 Hz; 5 V) at intervals of 4 min. ICP and MAP variations were documented by the PowerLab 26 T (ADInstruments, Sydney, Australia) system. The data was processed through LabChart 8 software (ADInstruments, Sydney, Australia).

### 2.5. Microarray analysis

The miRNA expression profile was investigated on three MSCs and

three MSC-Exos from rats. In a nutshell, total RNA was extracted from Exos and MSC using TRIzol (Invitrogen, Carlsbad, CA, USA). And the RNA quality was evaluated using an Agilent NanoDrop 2000 and 2100 BioAnalyzer. Using the Affymetrix GeneChip miRNA 4.0 Array (Santa Clara, CA, USA), the differential expression of miRNAs between MSCs and MSC-Exos was determined. The total RNA (200 ng) was labeled with the Affymetrix FlashTag Biotin HSR RNA Labelling Kit per the manufacturer's instructions. On a GeneChip Hybridization Oven 645, labeled samples were hybridized with the arrays. The samples were then rinsed with PBS and stained with the GeneChip Hybridization Wash and Stain Kit on a GeneChip Fluidics Station 450 using the GeneChip Hybridization Wash and Stain Kit before being viewed on an Affymetrix GeneChip Scanner 3000.

### 2.6. Bioinformatics analysis for microarray data

Differential expression analysis was performed between the MSCs and MSC-Exos groups using the Limma package to identify the differentially expressed miRNAs (DEMs) with a cutoff value of fold change (FC) $> 2$. A heatmap analysis of the top 20 DEMs with the highest FC was performed. Utilizing the TargetScan, miRWalk, and miRDB databases, the target genes of the top 20 DEMs were predicted. Fisher's exact test selected the target genes for Gene Ontology-Biological Process (GO-BP) and Kyoto Encyclopaedia of Genes and Genomes (KEGG) enrichment analysis. The threshold for statistical significance was defined at $p < 0.05$.

### 2.7. Cell transfection

CCSMCs from the third logarithmic phase passage were introduced into a six-well plate. Using LipofectamineTM 2000 (Invitrogen, Carlsbad, CA), CCSMCs were transfected with miR-296–5p mimics, miR-296–5p inhibitors, miR-337–3p mimics, miR-337–3p inhibitors, and negative control (NC).

### 2.8. Dual-luciferase reporter assay

Using a dual luciferase reporter assay, it was determined if PTEN was the target of miR-296–5p and miR-337. Briefly, the wild-type or mutant 3′ UTR sequences of PTEN were introduced into the Xba I and Fse I sites of the pGL3 vector (GeneChem, Shanghai, China). In 96-well plates, HEK293T cells were seeded and then transfected with miR-296–5p and miR-337–3p lentiviruses or negative control lentiviruses (miR-296–5p-NC and miR-337–3p-NC). Then, cells were co-transfected with 50 ng of pGL3 vector containing wild type or mutant 3′ UTR sequences of PTEN and 10 ng of pRL-TK vector using Lipofectamine LTX (Invitrogen, Carlsbad, CA). After 24 h, cells were harvested, and the firefly and Renilla luciferase activities were determined using Dual-luciferase Reporter Assay System Kits (Promega) and a Victor X machine (Perkin-Elmer, Boston, MA).

### 2.9. Real-time quantitative PCR (RT-qPCR)

Using the TRIzol (Invitrogen) Reagent, total RNA was extracted from the cells. PrimeScript RT reagent kit with gDNA Eraser (Takara, Japan) was utilized for reverse transcription procedures. Then, RT-qPCR was carried out utilizing the LightCycle 480 II PCR System (Rochester, USA) and a standard SYBR Green PCR reagent (Toyobo, Osaka, Japan). The U6 small RNA and β-actin were used as reference RNAs for miRNA and mRNA measurements. The $2^{-\Delta\Delta CT}$ method was utilized for relative gene expression level quantification. The RT-qPCR primer sequences are listed in Table 1.

### 2.10. Western blot assay

Euthanasia of animals was conducted 30 min after the assessment of ICP and MAP. The penises were separated into two parts perpendicular to the long axis at random, each with a comparable size and morphology. The Western blot experiment was performed on one tissue segment. Immunofluorescence staining and Masson's trichrome staining were performed using another tissue segment. Rat penises or CCSMCs were lysed in ice-cold radioimmunoprecipitation assay lysis buffer (Sigma-Aldrich) containing a protease inhibitor mixture (Sigma-Aldrich). Using a BCA protein assay reagent (ThermoFisher Scientific), the protein concentrations were accurately measured. 20 g of protein samples were separated by SDS-PAGE and transferred to a polyvinylidene difluoride membrane (Millipore, USA). The membrane was blocked for an hour with 5% skim milk before being incubated overnight at 4 °C with primary antibodies against β-actin (1:1000; 42 kDa, Santa Cruz Biotechnology), PTEN (1:2500; 47 kDa, Abcam), phospho-AKT (Thr308) (1:1000; 60 kDa, Cell signaling technology), phospho-AKT (Ser473) (1:5000; 56 kDa, Abcam), AKT(1:1000; 60 kDa, Cell signaling technology), phospho-eNOS (Ser1177) (1:1500; 133 kDa, Abcam), eNOS (1:750; 133 kDa, Abcam), alpha-smooth muscle actin (1:500; 42 kDa, Abcam), VEGFA (1:1000; 40 kDa, Proteintech), Caspase 3 (1:750; 35/17kDA, Cohesion Biosciences), Bcl-2 (1:1000; 26 kDa, Abcam), Bax (1:500; 20 kDa, Cell signaling technology). Following washes of the membrane three times, a secondary antibody labeled with horseradish peroxidase (HRP) was added and incubated with the membrane for one hour. After washing three times for 10 min with TBST, the protein bands were captured using the Fujifilm LAS-4000 Image Analyzer (Tokyo, Japan) and assessed using ImageJ software (NIH, USA).

**Table 1**
Primer sequences used for RT-qPCR.

| Gene | Primer Sequence (5′ to 3′) |
|---|---|
| miRNA-296–5p | Forward: GGACCTTTCTGGAGGGCCC<br>Reverse: GACACCTTCAGGAGAGCCTCC |
| miRNA-337–3p | Forward: AGTGTAGTGAGAAGTTGGGGGG<br>Reverse: TTGAAGGGGGTGAAGAAAGGCA |
| PTEN | Forward: GAAGACCATAACCCACCACAGC<br>Reverse: TTACACCAGTCCGTCCTTTCCC |

Abbreviations: miRNA-296–5p, microRNA-296–5p; miRNA-337–3p, microRNA-337–3p; PTEN, phosphatase and tensin homolog.
Figure legends

### 2.11. Masson's trichrome staining

In brief, the expression of smooth muscle and collagen fibrils in the corpus cavernosum was evaluated using a Masson trichrome stain reagent (Sigma-Aldrich). Smooth muscles were stained red, while collagenous fibers were stained blue. The software Image-Pro Plus 5.0 (Media Cybernetics, Inc., Bethesda, Maryland, United States) was utilized to analyze the smooth muscle-to-collagen ratio.

### 2.12. Immunofluorescence staining

The penile tissues were fixated with 4% paraformaldehyde and dehydrated with 30% sucrose in PBS overnight. Before the samples were mounted on glass transparencies, they were implanted and divided into 5 μm sections. The transparencies were incubated with primary antibodies against phospho-AKT (Thr308) (1:1000; 60 kDa; Cell signaling technology) and PTEN (1:2500; 47 kDa; Abcam) after an hour of immersion and blocking. The specimens were then rinsed and incubated with Alexa Fluor-594-conjugated secondary antibodies (Thermo Fisher Scientific). Nuclei were stained with DAPI (Cell Signalling Technology) for 5 min. Then the fluorescence signals of samples were observed under a fluorescence microscope (Nikon, Tokyo, Japan).

### 2.13. CCSMCs isolation and identification

CCSMCs were extracted from the penises of normal, 8-week-old male Sprague-Dawley rats using the protocols described in previous studies [26]. Then the CCSMCs were grown at 37 °C in a humidified environment of 5% $CO_2$ in Dulbecco's modified eagle medium (DMEM) containing 10% PBS, 1% penicillin, and 1% streptomycin. After achieving 80–90% confluence, primary CCSMCs were passed at a 1:3 ratio. At three to five passages, CCSMCs were identified by immunofluorescence staining with alpha-smooth muscle actin (α-SMA; Abcam, USA).

### 2.14. Cell viability assay

Using a CCK8 reagent (CK04, Dojindo, Kumamoto, Japan), CCSMCs from various treatment groups were collected and analyzed. The cells were then counted by measuring their optical density (OD) at 450 nm with a microplate reader (Victor 3, Pekin Elmer, USA). The rate of cell division was proportional to the optical density value. The experiments were repeated three times.

### 2.15. Apoptosis analysis by flow cytometry

Cell apoptotic analysis was carried out with an Annexin–V/FITC apoptosis kit (BD Biosciences, USA). In brief, CCSMCs were pre-incubated for 24 h with 50 μg Exos, 100 μg Exos, miR-296–5p and miR-337–3p mimic, and 100 μg Exos + 0.5 μmol AKT1/2 kinase inhibitor. The medium was then treated for 12 h with $H_2O_2$ at a final concentration of 50 μM. As a control, an equivalent volume of PBS was administered to the CCSMCs. To detect cell viability, the cells were rinsed twice with PBS, collected, and stained with Annexin V/propidium iodide (PI) in the dark for 15 min at 4 °C. The vitality of cells was determined using a flow cytometer (ACEA NovoCyte, USA) and the NovoExpress software (ACEA Biosciences).

### 2.16. Statistical analysis

The data presented in this study are the mean standard deviation. Per ARRIVE guidelines, the sample size was determined using PASS 15.0 (NCSS, Utah, USA). The analysis of two-group experiments was conducted using a two-tailed Student's t-test. Multiple group differences were analyzed using one-way analysis of variance (ANOVA) followed by Tukey–Kramer post hoc tests for multiple comparisons. All statistical analyses were performed using GraphPad Prism 8.0 (La Jolla, CA) and SPSS 26.0 (Chicago, IL, USA) software. If $p < 0.05$, differences are considered statistically significant.

## 3. Results

### 3.1. Characterization of MSC-Exos

The isolated particles were confirmed to be exosomes by examining their morphology and expression of exosomal markers. Under a transmission electron microscope (TEM), the exosomes were observed to have a round morphology (Fig. 1A). When MSCs and MSC-Exos were evaluated using Western blot, MSC-Exos tested strongly positive for exosome markers TSG101 and CD63 (Fig. 1B). NTA shows that most MSC-Exos have a diameter of approximately 100 nm (Fig. 1C). All of these results indicate that the separated particles are indeed Exos.

### 3.2. MSC-Exos effectively augment the erectile response in AED rats

Isolated MSC-Exos were injected into the corpus cavernosum of AED rats (Fig. 1D). Four weeks after injection, we detected ICP and MAP to assess the erectile response of rats in each group (Fig. 2A–H). The max ICP/MAP ratio and total ICP (area under curve) values were used to compare the erectile function of various groups (Fig. 2H and I). The results demonstrated a considerable decrease in max ICP/MAP and total ICP between AED rats and normal rats. After MSCs injection, the max ICP/MAP and total ICP values of the AED + MSCs group were significantly higher than those of the AED group. In contrast, the addition of the Exos inhibitor (GW4869, 10 μM, D1692, Sigma Aldrich) in the AED + MSC + Exos inhibitor group had no significant effect on max ICP/MAP or total ICP value relative to the AED group. It indicates that MSCs may restore erectile function in AED rats by secreting Exos. Furthermore, the AED + MSCs group showed limited improvement, whereas the AED + Exos group showed a more pronounced dose dependence of increases in max ICP, max MAP, and total ICP values. Adding an AKT1/2 kinase inhibitor in the AED + Exos 100 μg + AKTi group showed no significant effect on erectile function compared with the AED group, suggesting that Exos may improve erectile function by regulating the AKT signaling pathway. In addition, GW4869 and AKT1/2 kinase inhibitors were also injected alone into normal or AED rats to confirm the potential effect on erectile function. For a detailed description, see the supplemental materials (Fig. S1 A and B).

### 3.3. Exosomal miR-296–5p and miR-337–3p regulate the PTEN/PI3K/AKT signaling pathway

To further explain why MSC-Exos showed better therapeutic effects than MSCs, we conducted a microarray analysis for the miRNA expression profile. Based on the microarray results, 112 DEMs (6 upregulated and 106 downregulated) were found to be differentially expressed across the MSC-Exos and MSCs with a cutoff value of fold change (FC) $> 2$. The heatmap analysis shows the top 20 significant DEMs with the highest FC differences (Fig. 1E). The target genes of the top 20 DEMs were predicted by TargetScan, miRWalk, and miRDB databases; the result was depicted in a Venn diagram (Fig. 1F). The relative expressions of miR-296–5p and miR-337–3p in the MSCs and MSC-Exos are seen in Fig. S2. PTEN is one of the target genes regulated by miR-296–5p and miR-337–3p (Fig. 1F). KEGG pathway analysis revealed enrichment for the PI3K-AKT signaling pathway and cellular senescence (Fig. 1G). These target genes were also enriched for GO-BP terms related to positive regulation of nitric-oxide synthase activity, nitric oxide biosynthesis, and smooth muscle cell proliferation (Fig. 1H). To determine whether miR-296–5p and miR-337–3p directly bind to the PTEN 3′ UTR, the wild-type or mutant 3′ UTR target sequences (Fig. 3B) were cloned into the luciferase reporter vector pGL3 and transfected into cells using the reference vector pRL-TK. The findings indicate that miR-296–5p and miR-337–3p suppress the luciferase activity of the wild-type PTEN 3′UTR (Fig. 3C and D). In order to validate whether miR-296–5p and miR-337–3p regulate the PTEN/PI3K/AKT signaling pathway, CCSMCs were transfected with mimics, inhibitors, and NC of miR-296–5p or miR-337–3p. The expression of miR-296–5p and miR-337–3p were increased after being transfected with mimics and decreased after being transfected with inhibitors (Fig. 3E). The mRNA level of PTEN corroborated the results that miR-296–5p and miR-337–3p negatively regulate PTEN expression (Fig. 3F). The Western blot results also demonstrated that mimics of miR-296–5p or miR-337–3p downregulated PTEN expression and upregulated AKT expression (Fig. 3G–I). In contrast, inhibitors of miR-296–5p or miR-337–3p upregulated PTEN expression and downregulated AKT expression (Fig. 3 G–I). These results reveal that miR-296–5p and miR-337–3p directly bind to PTEN and regulate the PTEN/PI3K/AKT signaling pathway.

### 3.4. The miR-296–5p and miR-337–3p levels are reduced in AED rats, while miR-296–5p and miR-337–3p transfection ameliorate AED

The levels of miR-296–5p and miR-337–3p expression are decreased in the penises of AED rats (Fig. 3A). It suggests that the decrease of miR-296–5p and miR-337–3p may be one of the causes of AED. To verify the role of miR-296–5p and miR-337–3p in AED, in vivo experiments were performed. The lentiviruses loaded with miR-296–5p or miR-337–3p

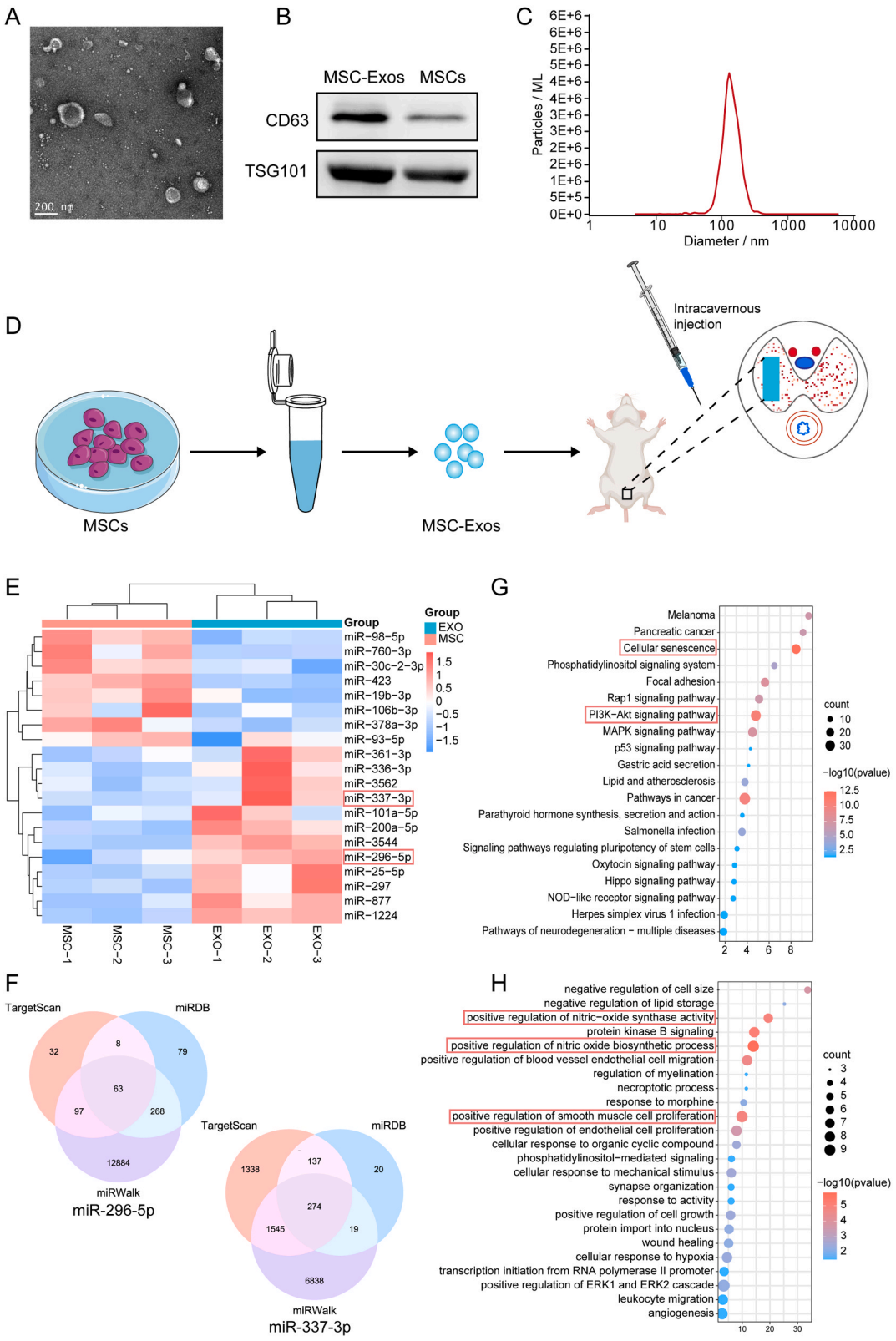


**Fig. 1.** Identification and microarray analysis of MSC-Exos and bioinformatics analysis for microarray data. (A) Representative transmission electron micrographs of MSC-Exos with a round shape. Scale bar = 200 nm. (B) Western blot assay indicating positive expression for the CD63 and TSG101 in MSC-Exos, and weakly positive in MSCs. (C) NTA revealed the particle diameters of most MSC-Exos are approximately 100 nm. (D) The schematic diagram of the preparation and administration of MSC-Exos. (E) The top 20 DEMs between Exos and MSCs based on the microarray data were visualized on a heatmap. (F) Venn diagram of miR-296–5p and miR-337–3p target genes predicted by Targetscan, miRWalk, and miRDB databases. (G) KEGG pathway enrichment analysis for target genes. (H) GO-BP enrichment analysis for target genes.

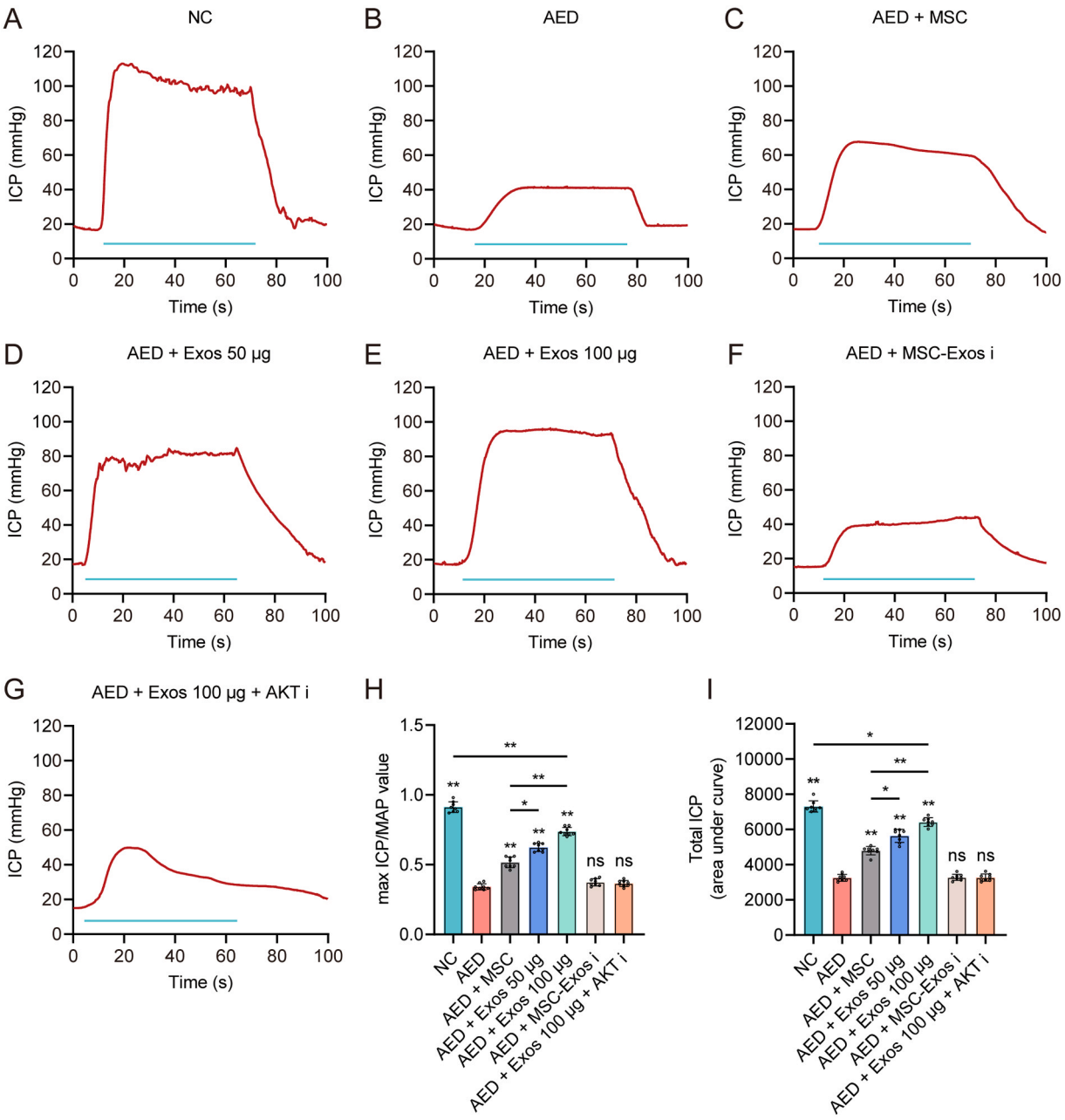


**Fig. 2.** Erectile responses of rats after treatment. (A–G) ICP values were measured to evaluate the erectile functions in each group. The colored lines denote electrical stimulation of the cavernous nerve for 60 s (H) Ratios of maximum ICP to MAP derived from each group are presented as bar graphs, and the data are shown as mean ± standard deviation. (I) The total ICP is obtained by calculating the area under curve, and the data are shown as mean ± standard deviation. *$p < 0.05$; **$p < 0.01$ vs. AED group; ns: no significant difference.

($1 \times 10^9$ TU/ml, 20 μl) were injected into the corpus cavernosum of AED rats for the transfection groups, respectively; empty vectors were injected into AED rats for the control AED group. After 3 weeks, ICP and MAP values were measured for each rat. The results show that intracavernous injection of miR-296–5p and miR-337–3p restores erectile function in AED rats (Fig. 3J and K).

### 3.5. MSC-Exos enhance erectile function in AED rats by regulating the PTEN/PI3K/AKT signaling pathway and inhibiting apoptosis

To identify whether MSC-Exos alleviate AED by modulating the PTEN/PI3K/AKT signaling pathway and diminishing apoptosis, protein expressions related to the PTEN/PI3K/AKT pathway and apoptosis in AED treatment groups were detected by Western blot. The results indicated the expression levels of p-AKT-thr308, p-AKT-ser473, p-eNOS, α-SMA, VEGFA, and Bcl-2 in the MSCs, Exos 50 μg, and Exos 100 μg groups were increased significantly compared to the PBS group. In contrast, the effect could be reversed following treatment with the Exos inhibitor or AKT1/2 kinase inhibitor (Fig. 4A–C). In contrast, the expression levels of PTEN, cleaved-Caspase 3 and Bax showed an opposite trend (Fig. 4A and C). In addition, the protein expressions of p-AKT-thr308, p-AKT-ser473, p-eNOS, α-SMA, VEGFA, and Bcl-2 were significantly increased in the Exos 100 μg group compared to the MSCs group. In contrast, protein expressions of PTEN, cleaved-Caspase 3 and Bax attenuated dramatically in the Exos 100 μg group than in the MSCs group (Fig. 4A and C). These findings were further supported by immunofluorescence staining for PTEN and AKT (Fig. 5C–F). These results reveal that MSC-Exos enhance erectile function in AED rats via

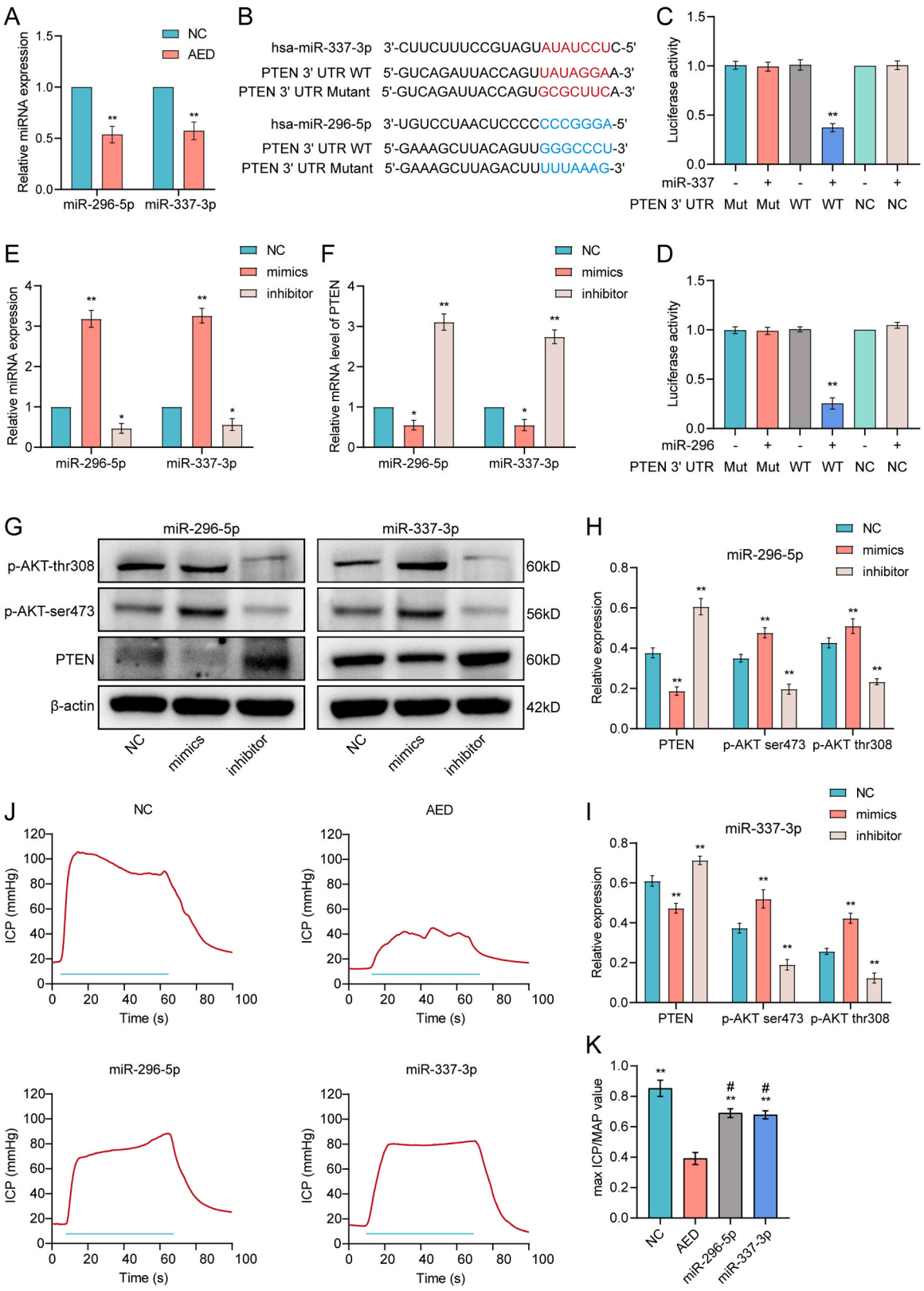


**Fig. 3.** MiR-296–5p and miR-337–3p directly suppress the expression of PTEN to regulate the AKT pathway. (A) The expression levels of miR-296–5p and miR-337–3p were down-regulated in AED rat penile tissues compared with normal rat penile tissues. (B) Potential miR-296–5p and miR-337–3p binding sites in the PTEN 3′ UTR. (C and D) Dual-luciferase reporter assay revealed that PTEN 3′ UTR activity was inhibited by miR-296–5p and miR-337–3p. (E) CCSMCs were transfected with miR-296–5p mimics, miR-296–5p inhibitor, miR-337–3p mimics, miR-337–3p inhibitor, and negative control (NC); expression levels of miR-296–5p and miR-337–3p were successfully increased after transfected with mimics but repressed after transfected with inhibitor. (F) Overexpression of miR-296–5p and miR-337–3p inhibited mRNA levels of PTEN. (G–I) Western blot assay revealed that overexpression of miR-296–5p and miR-337–3p resulted in downregulation of PTEN and upregulation of phospho-AKT (Thr308 and Ser473). (J and K) Intracavernous injection of miR-296–5p and miR-337–3p improved erectile function in AED rats.

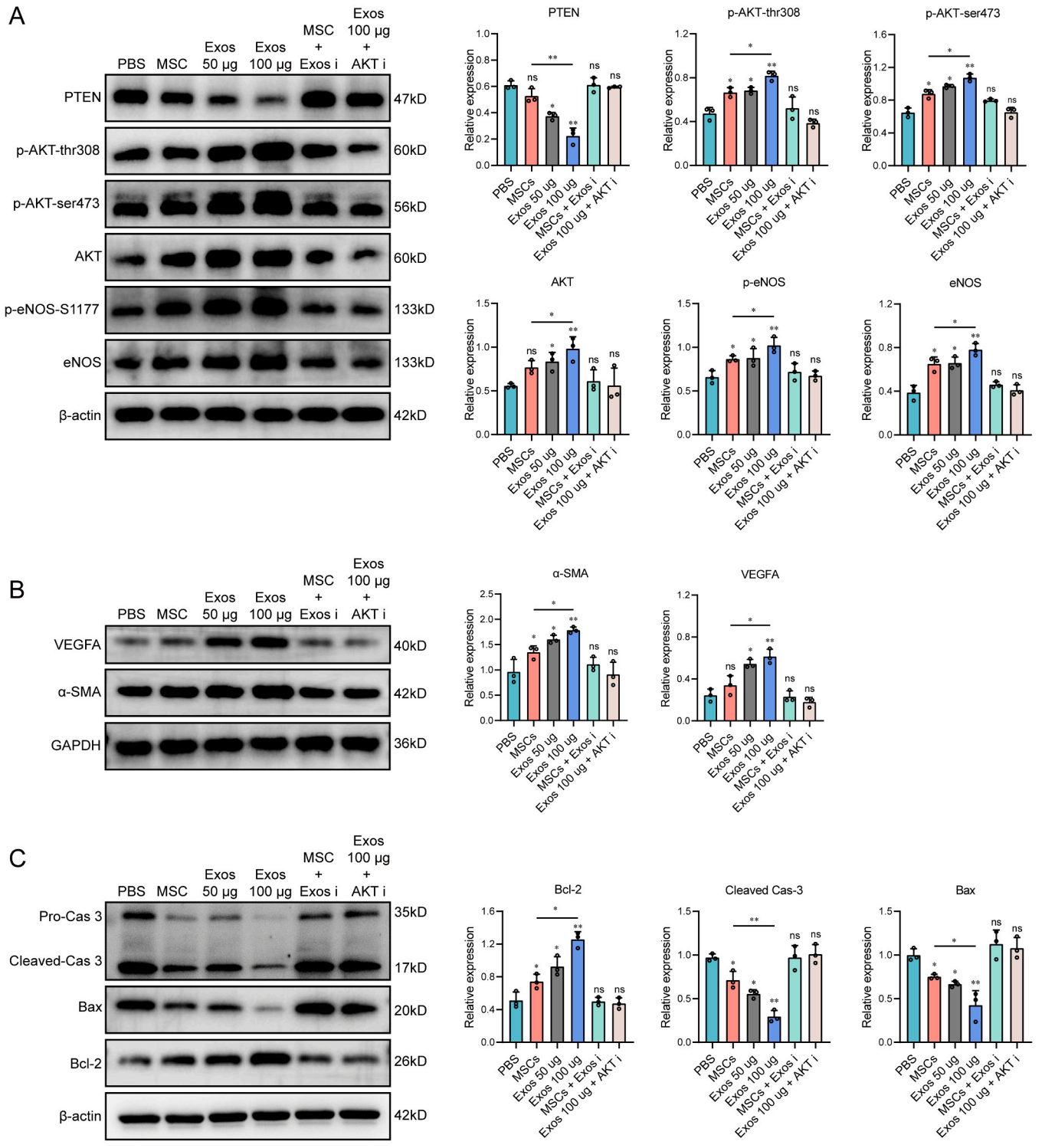


**Fig. 4.** MSC-Exos ameliorated AED by regulating the PTEN/PI3K/AKT pathway and inhibiting apoptosis. (A–C) Representative images of western blots for protein expression of PTEN/PI3K/AKT/eNOS pathway, Caspase 3, Bax, Bcl-2, α-SMA, and VEGFA from each group. Data are displayed as the relative density versus β-actin. $^{*}p < 0.05$, $^{**}p < 0.01$ vs. AED group; ns: no significant difference.

modulating the PTEN/PI3K/AKT signaling pathway and reducing apoptosis. The serum miR-296–5p and miR-337–3p levels in AED rats showed no significant changes after 100 μg MSC-Exos injection (Fig. S3).

### 3.6. MSC-Exos restore the histological structure of the corpus cavernosum

After 4 weeks of injection, histological changes were evaluated with Masson's trichrome (Fig. 5A and B). When compared to the NC group, the ratios of smooth muscle to collagen were considerably decreased in the AED group (Fig. 5A and B). After treatment with MSCs, Exos 50 μg, and Exos 100 μg, the ratios of smooth muscle to collagen were noticeably restored (Fig. 5A and B). However, 100 μg Exos treatment performed better than MSCs treatment (Fig. 5A and B). The effects of MSCs and Exos on the ratios of smooth muscle to collagen could be reversed by

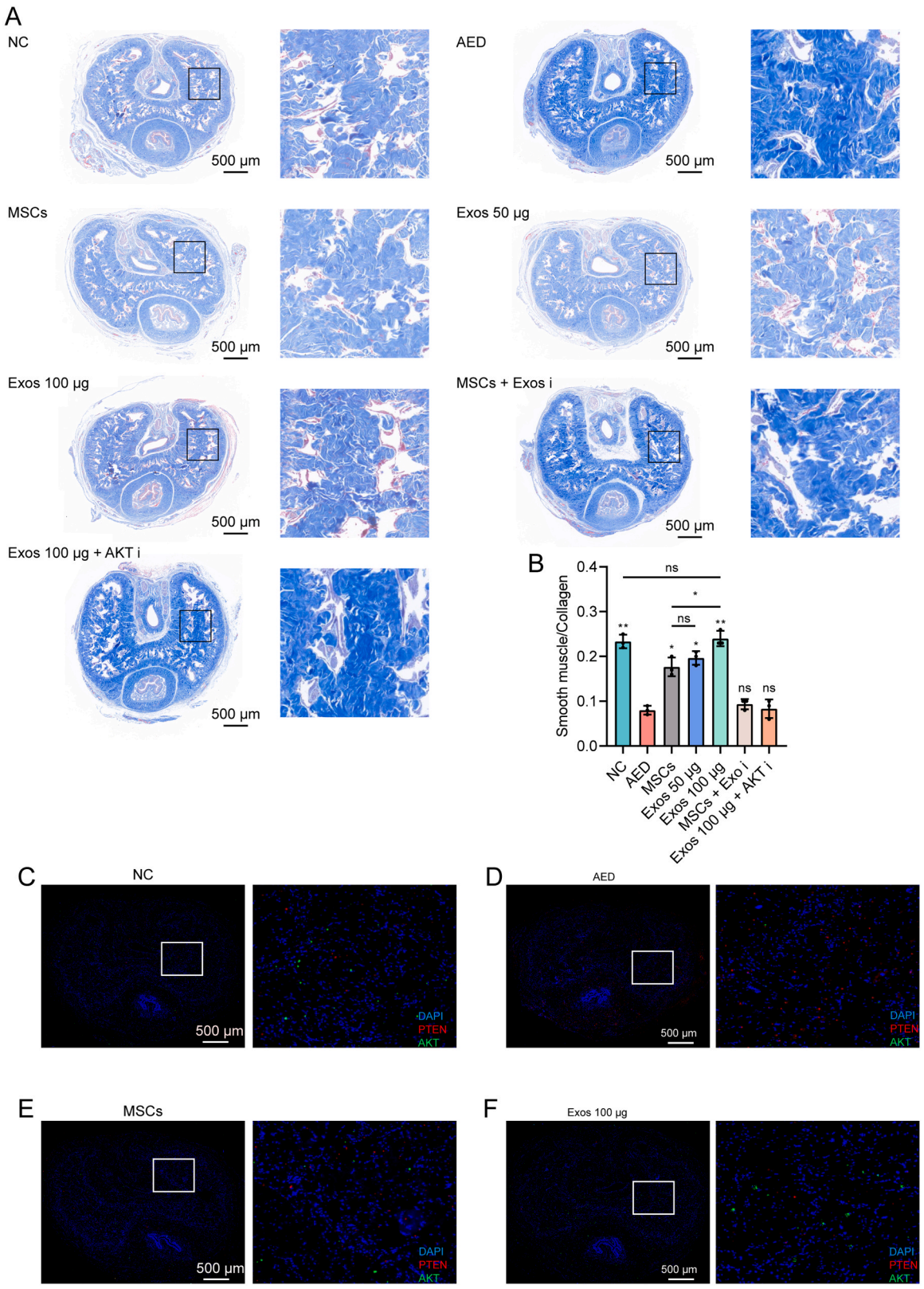


**Fig. 5.** Effect of MSC-Exos on the histological structure of the corpus cavernosum and immunofluorescence staining for PTEN and AKT. (A) Masson's trichrome staining of penile tissue from different groups after treatment. The smooth muscle is stained red, while the collagen is stained blue. (B) Data are displayed as the ratio of smooth muscle to collagen. * $p < 0.05$, ** $p < 0.01$ vs. AED group; ns: no significant difference. (C–F) Representative immunofluorescence staining shows expressions of PTEN (green fluorescence) and AKT (red fluorescence) in NC, AED, MSCs, and Exos100 μg groups.

the Exos inhibitor or AKT1/2 kinase inhibitor (Fig. 5A and B). These findings suggest that MSC-Exos restore the histological structure of the corpus cavernosum by improving the ratios of smooth muscle to collagen.

### 3.7. MSC-Exos protect CCSMCs from apoptosis

We investigated the role of MSC-Exos in vitro further. CCSMCs were isolated from normal rat penises (Fig. 6A) and characterized with immunofluorescence staining for α-SMA (Fig. 6B). The CCK8 assay was used to confirm the effects of MSCs or Exos co-culture on the proliferation of CCSMCs (Fig. 6C). Cell viability was promoted after treatment with MSCs or Exos, and the effect could be entirely reversed by GW4869 and partially reversed by the AKT1/2 kinase inhibitor (Fig. 6C). GW4869 or AKT1/2 kinase inhibitor alone did not affect cell viability (Fig. 6C). CCSMCs were incubated with PBS, Exos 50 μg, Exos 100 μg, mimics, and Exos 100 μg + AKT1/2 kinase inhibitor for 6 h. The cells were then treated for 18 h with $H_2O_2$ to induce apoptosis. The cells were stained with Annexin V-FITC/PI and analyzed by flow cytometry (Fig. 6D and E). After $H_2O_2$ treatment, the proportion of apoptotic cells was 19.8% ± 0.91 when cells were incubated without Exos. When cells were incubated with Exos, however, the proportion of apoptotic cells was 14.5% ± 1.14 (50 μg) and 8.4% ± 1.09 (100 μg). But the effect of Exos could be reversed partially by the AKT AKT1/2 kinase inhibitor (Fig. 6E). Therefore, we are prone to speculate that Exos protect CCSMCs from apoptosis, at least in part, via the PTEN/PI3K/AKT signaling pathway.

## 4. Discussion

AED continues to be a global health concern, with epidemiological studies revealing a 52% prevalence of mild to moderate ED in men aged

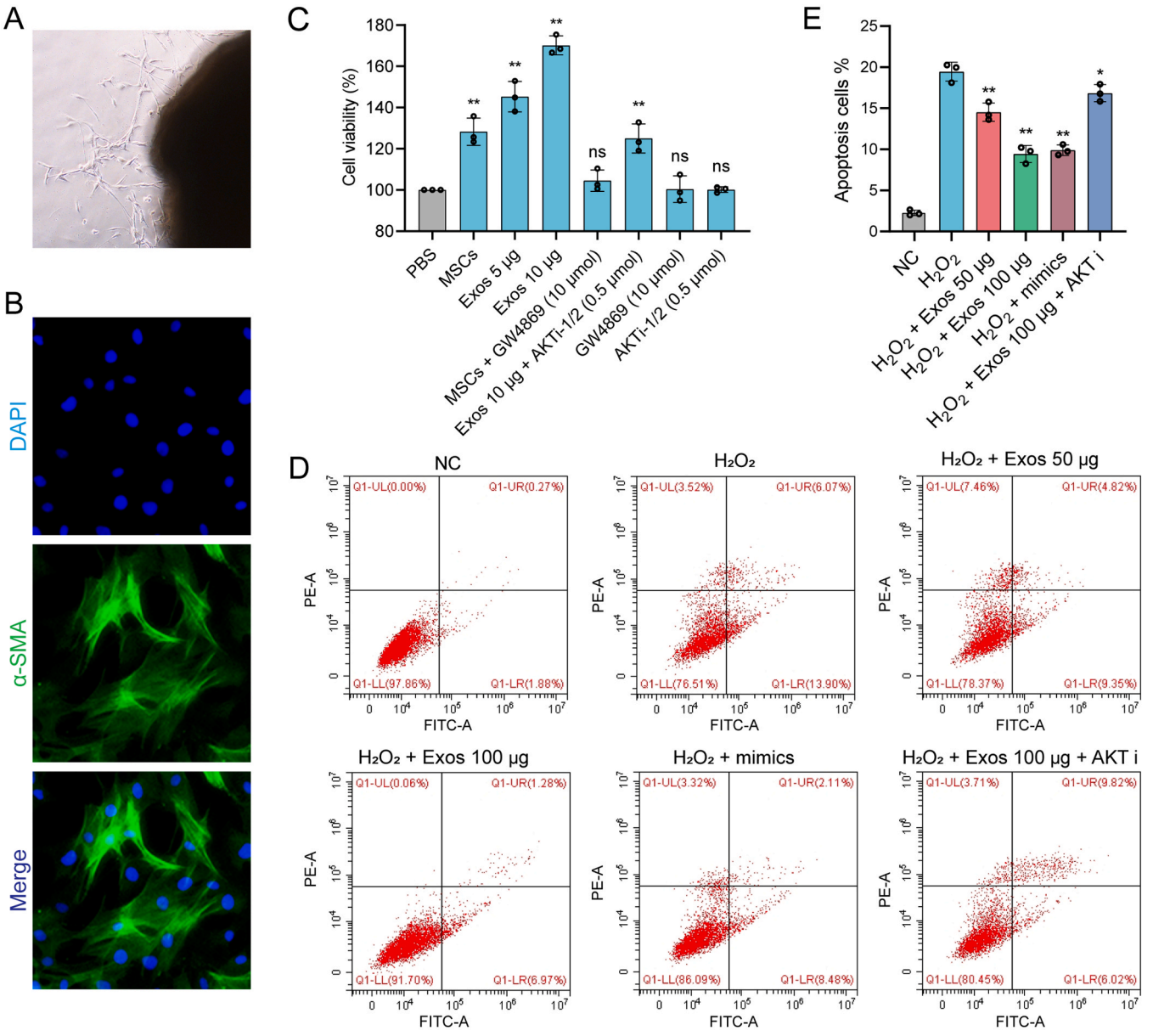


**Fig. 6.** Effect of MSC-Exos on CCSMCs apoptosis. (A) Primary CCSMCs emerge from the corpus cavernosum tissue after 5 days of culture. (B) CCSMCs identification was conducted by immunofluorescence staining of α-SMA, × 40 amplification. (C) CCK8 assay showed MSCs or Exos co-culture promoted the proliferation of CCSMCs. (D) Cell viability was detected by flow cytometry in the normal control group treated with PBS (NC) and the $H_2O_2$-treated groups (pretreated with PBS, Exos 50 μg, Exos 100 μg, mimics, and Exos 100 μg + AKT1/2 kinase inhibitor). (E) The average apoptotic cell percentages in each group. *$p < 0.05$; **$p < 0.01$; ns: no significant difference.

40–70 [27]. Drug therapy is a common form of treatment, but its therapeutic efficacy is unsatisfactory. Therefore, more effective treatments for AED are required. MSC therapy has provided a new perspective on the treatment of AED in recent years. However, large-scale implementation was restricted due to the potential risk of injecting living cells. A growing body of evidence indicates that the functional benefits of MSCs are primarily mediated by paracrine activity [28]. Paracrine factors such as exosomes seem to be a better treatment alternative. The present study first identifies that MSC-Exos markedly attenuate AED by delivering miR-296–5p and miR-337–3p to regulate the PTEN/PI3-K/AKT signaling pathway. Furthermore, exosomes also inhibited the apoptosis of CCSMCs by diminishing oxidative stress.

The discovery of exosomes provides important insights into the mode of intercellular communication [29], involving multiple physiologic and pathologic processes, including angiogenesis [30], immunomodulation [31], tissue repair [32], fibrosis [33], and apoptosis [34]. Along with secreting soluble factors such as cytokines, exosomes work primarily by horizontally transferring mRNAs, miRNAs, and proteins, which subsequently affect the activity of target cells in multiple ways [35]. Exosomes have been confirmed to improve diabetes mellitus-related ED by inhibiting fibrosis and cell apoptosis and increasing smooth muscle content [36,37]. Besides that, exosomes have been proven to be increasingly implicated in the aging process and exert an anti-senescence role when secreted from stem cells [38]. Exosome-mediated cell-free therapies have a range of advantages over other cell therapies. (i) they can be conserved at 80 °C for more than 6 months without any cryoprotectant chemicals but are still functioning [39], (ii) they are encapsulated in the phospholipid bilayers that preserve their contents, allowing them to travel vast distances across tissues [40], and (iii) the use of the exosomes addresses various potential safety concerns involved with the transplantation of live or proliferative cell populations, such as immunological tolerance, tumorigenicity, and infection acquisition [41]. The application of exosome-mediated cell--free therapies appears to be the subject of intense research as an innovative replacement for whole-cell therapy. Several investigations have shown that the implantation duration of MSCs is frequently insufficient to exert a meaningful therapeutic effect [42,43]. It has been observed that < 1% of MSCs survive transplantation for more than one week [44], indicating that the major actions of MSCs are possibly mediated via paracrine pathways [45]. This evidence supports our findings that MSC-Exos treatment has a better effect on AED than MSC therapy. To explain the apparent discrepancy, we conducted miRNA sequencing in MSCs and MSC-Exos. The results show that miR-296–5p and miR-337–3p are significant differential miRNAs, suggesting MSC-Exos might play a role partially through the delivery of miR-296–5p and miR-337–3p to recipient cells.

Recently, ample evidence implicates miRNAs in serving critical roles in regulating development and tissue homeostasis; miRNA dysregulation has been linked to the pathophysiology of a variety of diseases, including cancer, cardiovascular, neurodegenerative, and age-related disorders [46–48]. However, the role of miRNAs in AED is complex. It has been shown that miRNA-145-engineered MSCs improve erectile dysfunction in aged rats [9]. The up-regulation of miRNA-200a has been proven to attenuate endothelial function and age-related erectile function [24]. In this study, it was discovered that miR-296–5p and miR-337–3p are downregulated in the penile of aged rats. Multiple studies have linked miRNA-296–5p to a variety of human diseases, including malignancy, hypertension, and type 2 diabetes [49–51]. These pathologic changes are also involved in age-related disorders. Similarly, miR-337–3p is also identified to ameliorate hyperlipemia and osteoarthritis by reducing serum low-density lipoprotein cholesterol (LDL-C) and inhibiting oxidative stress and apoptosis [52,53]. As such, given the main processes that they participate in, we believe that exosomal miR-296–5p and miR-337–3p mediate at least part of the therapeutic effects of MSC-Exos on AED.

To elaborate further on the mechanism of MSC-Exos-mediated enhancement in AED, a pathway enrichment analysis was performed on the predicted target genes of miR-296–5p and miR-337–5p. We found that the exosomal miR-296–5p and miR-337–3p target and inhibit PTEN. PTEN is known as a dual-specific phosphatase that dephosphorylates lipid and protein substrates, ultimately antagonizing the PI3K/AKT signaling pathway [54]. It has been reported that the PTEN/AKT pathway plays a crucial role in developing diabetic ED and portrays potential tractable therapeutic targets [55]. The downstream signaling endothelial nitric oxide synthase (eNOS)/nitric oxide (NO) pathway modulated by the PI3K/AKT pathway represents a key feature in corpus cavernosal smooth muscle relaxation during penile erection [56]. A previous study showed that human tissue kallikrein 1 improves AED by upregulating the PI3K/AKT pathway. In addition to this, the PI3K/AKT pathway has been shown to be implicit in ED induced by diabetes mellitus or cavernous nerve damage [57,58]. These studies corroborate our findings that exosomal miR-296–5p and miR-337–3p improve AED by targeting and silencing PTEN, which regulates the PI3K/AKT pathway and downstream eNOS/NO signaling (Fig. 7).

Furthermore, a normal penile erection requires a suitable quantity of relaxed smooth muscle. An insufficiency of CCSMC causes veno-occlusive dysfunction and exacerbates ED symptoms [59]. During the aging process, smooth muscle reduction and collagen deposition occur in the cavernosa [60]. As indicated in a previous study, MSC-Exos promote smooth muscle restoration and erectile response [21]. Moreover, apoptosis induced by OS reduces endothelial cells and smooth muscles, leading to impairment in cavernous hemodynamics and penile erectile failure in AED patients [61]. The Bax/Bcl-2 families are well-understood cellular proteins responsible for the regulation of apoptosis; overexpression of Bax induces apoptosis, whereas Bcl-2 suppresses apoptosis. Existing evidence indicates restoring the balance between Bax and Bcl-2 protects CCSMCs from apoptosis in AED [62]. Another study also validates our results that MSC-Exos improve ED by diminishing apoptosis of CCSMCs [63].

However, several limitations of our study should also be considered. We only determined the differential expression of miR-296–5p and miR-337–3p between normal and aged rats. More detailed miRNA expression profiling should be conducted in the penile tissue of normal and aged rats for a more comprehensive appreciation of the mechanisms of AED and its potential therapeutic targets. Another limitation of this study is that only animal experiments were conducted, and the effect of MSC-Exos on AED patients is unknown. Further efforts to translate MSC-Exos-mediated cell-free therapy into the clinical setting are needed.

In conclusion, our study proves that MSC-Exos alleviate AED by delivering miR-296–5p and miR-337–3p to regulate the PTEN/PI3K/AKT signaling pathway and inhibit the apoptosis of CCSMCs. It is believed that MSC-Exos hold great promise for cell-free therapeutic applications in age-related erectile dysfunction.

## Funding

The authors acknowledge the support from the National Natural Science Foundation of China (Grant No. 81873830, 82071635), Shandong Provincial Natural Science Foundation (ZR2023MH019), Shandong Traditional Chinese Medicine Technology Project (M-2022209), Shandong Province Medical and health development Plan (Grant No. 202004051394), Jinan Science and Technology Plan (Grant No. 202134010), National Health Commission medical and Health Development Plan (Grant No. HDSL2020010640), Jinan new colleges and universities 20 projects (Grant No. 2021GXRC085), Academic Promotion Programme (2020LI001) of Shandong First Medical University.

## CRediT authorship contribution statement

**Kefan Li:** Conceptualization; Methodology; Data curation; Writing-Original draft preparation. **Ruiyu Li**: Software; Data curation. **Zongyong Zhao:** Visualization; Investigation. **Chen Feng:** Software; Data

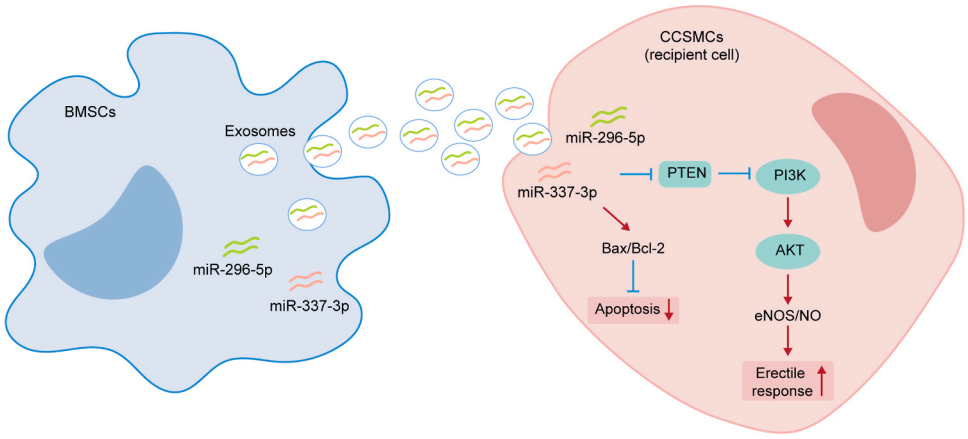


**Fig. 7.** Schematic representation of the regulatory role of MSCs-derived exosomal miR-296–5p and miR-337–3p in AED by modulating the PTEN/PI3K/AKT signaling pathway and inhibiting apoptosis of CCSMCs.

curation. **Shuai Liu:** Funding acquisition; Methodology; Resources; Supervision; Validation. **Qiang Fu:** Funding acquisition; Writing - review & editing; Supervision.

## Declaration of Competing Interest

The authors declare that they have no known competing financial interests or personal relationships that could have appeared to influence the work reported in this paper.

## Data Availability

All data generated or analyzed during this study are included in this work and are accessible upon request from the authors.

## Acknowledgments

Thanks for the support of Engineering Laboratory of Urinary Organ and Functional Reconstruction of Shandong Province, Shandong Provincial Hospital affiliated to Shandong First Medical University, Jinan, China. Partial images of Fig. 1D are obtained from BioRender (https://biorender.com/).

## Appendix A. Supporting information

Supplementary data associated with this article can be found in the online version at doi:10.1016/j.biopha.2023.115449.

## References

[1] I.A. Ayta, J.B. McKinlay, R.J. Krane, The likely worldwide increase in erectile dysfunction between 1995 and 2025 and some possible policy consequences, BJU Int. 84 (1999) 50–56, https://doi.org/10.1046/j.1464-410x.1999.00142.x.
[2] A. Ponholzer, C. Temml, K. Mock, et al., Prevalence and risk factors for erectile dysfunction in 2869 men using a validated questionnaire, 80-5; discussion, Eur. Urol. 47 (2005) 85–86, https://doi.org/10.1016/j.eururo.2004.08.017.
[3] A. Nicolosi, D.B. Glasser, S.C. Kim, et al., Sexual behaviour and dysfunction and help-seeking patterns in adults aged 40-80 years in the urban population of Asian countries, BJU Int. 95 (2005) 609–614, https://doi.org/10.1111/j.1464-410X.2005.05348.x.
[4] J. Haczynski, Z. Lew-Starowicz, B. Darewicz, et al., The prevalence of erectile dysfunction in men visiting outpatient clinics, Int. J. Impot Res. 18 (2006) 359–363, https://doi.org/10.1038/sj.ijir.3901435.
[5] N. Eser, A. Yoldaş, A. Yigin, et al., The protective effect of Ferula elaeochytris on age-related erectile dysfunction, J. Ethnopharmacol. 258 (2020), 112921, https://doi.org/10.1016/j.jep.2020.112921.
[6] R. Sadovsky, T. Miller, M. Moskowitz, et al., Three-year update of sildenafil citrate (Viagra) efficacy and safety, Int. J. Clin. Pr. 55 (2001) 115–128.
[7] M. Albersen, H. Orabi, T.F. Lue, Evaluation and treatment of erectile dysfunction in the aging male: a mini-review, Gerontology 58 (2012) 3–14, https://doi.org/10.1159/000329598.
[8] G. Lin, N. Hayashi, R. Carrion, et al., Improving erectile function by silencing phosphodiesterase-5, J. Urol. 174 (2005) 1142–1148, https://doi.org/10.1097/01.ju.0000168615.37949.45.
[9] Q. Liu, Y. Cui, H. Lin, et al., MicroRNA-145 engineered bone marrow-derived mesenchymal stem cells alleviated erectile dysfunction in aged rats, Stem Cell Res. Ther. 10 (2019) 398, https://doi.org/10.1186/s13287-019-1509-1.
[10] U. Milenkovic, M. Albersen, F. Castiglione, The mechanisms and potential of stem cell therapy for penile fibrosis, Nat. Rev. Urol. 16 (2019) 79–97, https://doi.org/10.1038/s41585-018-0109-7.
[11] G. Chamberlain, J. Fox, B. Ashton, et al., Concise review: mesenchymal stem cells: their phenotype, differentiation capacity, immunological features, and potential for homing, Stem Cells 25 (2007) 2739–2749, https://doi.org/10.1634/stemcells.2007-0197.
[12] Y. Zhu, T. Liu, K. Song, et al., Adipose-derived stem cell: a better stem cell than BMSC, Cell Biochem. Funct. 26 (2008) 664–675, https://doi.org/10.1002/cbf.1488.
[13] D.G. Phinney, M.F. Pittenger, Concise review: MSC-derived exosomes for cell-free therapy, Stem Cells 35 (2017) 851–858, https://doi.org/10.1002/stem.2575.
[14] I. Mahmud, T.J. Garrett, Mass spectrometry techniques in emerging pathogens studies: COVID-19 perspectives, J. Am. Soc. Mass Spectrom. 31 (2020) 2013–2024, https://doi.org/10.1021/jasms.0c00238.
[15] B. Yu, X. Zhang, X. Li, Exosomes derived from mesenchymal stem cells, Int. J. Mol. Sci. 15 (2014) 4142–4157, https://doi.org/10.3390/ijms15034142.
[16] A. Takahashi, R. Okada, K. Nagao, et al., Exosomes maintain cellular homeostasis by excreting harmful DNA from cells, Nat. Commun. 8 (2017) 15287, https://doi.org/10.1038/ncomms15287.
[17] S.W. Ferguson, J. Nguyen, Exosomes as therapeutics: the implications of molecular composition and exosomal heterogeneity, J. Control Release 228 (2016) 179–190, https://doi.org/10.1016/j.jconrel.2016.02.037.
[18] M. Ahmadi, J. Rezaie, Ageing and mesenchymal stem cells derived exosomes: molecular insight and challenges, Cell Biochem. Funct. 39 (2021) 60–66, https://doi.org/10.1002/cbf.3602.
[19] F. Chen, H. Zhang, Z. Wang, et al., Adipose-derived stem cell-derived exosomes ameliorate erectile dysfunction in a rat model of type 2 diabetes, J. Sex. Med. 14 (2017) 1084–1094, https://doi.org/10.1016/j.jsxm.2017.07.005.
[20] M. Li, H. Lei, Y. Xu, et al., Exosomes derived from mesenchymal stem cells exert therapeutic effect in a rat model of cavernous nerves injury, Andrology 6 (2018) 927–935, https://doi.org/10.1111/andr.12519.
[21] W. Huo, Y. Li, Y. Zhang, et al., Mesenchymal stem cells-derived exosomal microRNA-21-5p downregulates PDCD4 and ameliorates erectile dysfunction in a rat model of diabetes mellitus, Faseb J. 34 (2020) 13345–13360, https://doi.org/10.1096/fj.202000102RR.
[22] D.P. Bartel, MicroRNAs: genomics, biogenesis, mechanism, and function, Cell 116 (2004) 281–297, https://doi.org/10.1016/s0092-8674(04)00045-5.
[23] L.H. Chen, G.Y. Chiou, Y.W. Chen, et al., MicroRNA and aging: a novel modulator in regulating the aging network, Ageing Res. Rev. 9 (Suppl 1) (2010) S59–S66, https://doi.org/10.1016/j.arr.2010.08.002.
[24] F. Pan, X.F. Qiu, W. Yu, et al., MicroRNA-200a is up-regulated in aged rats with erectile dysfunction and could attenuate endothelial function via SIRT1 inhibition, Asian J. Androl. 18 (2016) 74–79, https://doi.org/10.4103/1008-682x.154991.
[25] Y. Liu, S. Zhao, L. Luo, et al., Mesenchymal stem cell-derived exosomes ameliorate erection by reducing oxidative stress damage of corpus cavernosum in a rat model of artery injury, J. Cell Mol. Med. 23 (2019) 7462–7473, https://doi.org/10.1111/jcmm.14615.
[26] J. Yang, Y. Zhang, G. Zang, et al., Adipose-derived stem cells improve erectile function partially through the secretion of IGF-1, bFGF, and VEGF in aged rats, Andrology 6 (2018) 498–509, https://doi.org/10.1111/andr.12483.
[27] H.A. Feldman, I. Goldstein, D.G. Hatzichristou, et al., Impotence and its medical and psychosocial correlates: results of the Massachusetts Male Aging Study, J. Urol. 151 (1994) 54–61, https://doi.org/10.1016/s0022-5347(17)34871-1.

[28] P.C. Dinh, D. Paudel, H. Brochu, et al., Inhalation of lung spheroid cell secretome and exosomes promotes lung repair in pulmonary fibrosis, Nat. Commun. 11 (2020) 1064, https://doi.org/10.1038/s41467-020-14344-7.
[29] X. Kou, X. Xu, C. Chen, et al., The Fas/Fap-1/Cav-1 complex regulates IL-1RA secretion in mesenchymal stem cells to accelerate wound healing, Sci. Transl. Med. 10 (2018), https://doi.org/10.1126/scitranslmed.aai8524.
[30] A. Shabbir, A. Cox, L. Rodriguez-Menocal, et al., Mesenchymal stem cell exosomes induce proliferation and migration of normal and chronic wound fibroblasts, and enhance angiogenesis in vitro, Stem Cells Dev. 24 (2015) 1635–1647, https://doi.org/10.1089/scd.2014.0316.
[31] J. Yang, X.X. Liu, H. Fan, et al., Extracellular vesicles derived from bone marrow mesenchymal stem cells protect against experimental colitis via attenuating colon inflammation, oxidative stress and apoptosis, PLoS One 10 (2015), e0140551, https://doi.org/10.1371/journal.pone.0140551.
[32] B. Zhang, M. Wang, A. Gong, et al., HucMSC-exosome mediated-wnt4 signaling is required for cutaneous wound healing, Stem Cells 33 (2015) 2158–2168, https://doi.org/10.1002/stem.1771.
[33] J. Guiot, M. Cambier, A. Boeckx, et al., Macrophage-derived exosomes attenuate fibrosis in airway epithelial cells through delivery of antifibrotic miR-142-3p, Thorax 75 (2020) 870–881, https://doi.org/10.1136/thoraxjnl-2019-214077.
[34] S. Zhang, S.J. Chuah, R.C. Lai, et al., MSC exosomes mediate cartilage repair by enhancing proliferation, attenuating apoptosis and modulating immune reactivity, Biomaterials 156 (2018) 16–27, https://doi.org/10.1016/j.biomaterials.2017.11.028.
[35] S. Tomasoni, L. Longaretti, C. Rota, et al., Transfer of growth factor receptor mRNA via exosomes unravels the regenerative effect of mesenchymal stem cells, Stem Cells Dev. 22 (2013) 772–780, https://doi.org/10.1089/scd.2012.0266.
[36] J. Song, T. Sun, Z. Tang, et al., Exosomes derived from smooth muscle cells ameliorate diabetes-induced erectile dysfunction by inhibiting fibrosis and modulating the NO/cGMP pathway, J. Cell Mol. Med. 24 (2020) 13289–13302, https://doi.org/10.1111/jcmm.15946.
[37] L.L. Zhu, X. Huang, W. Yu, et al., Transplantation of adipose tissue-derived stem cell-derived exosomes ameliorates erectile function in diabetic rats, Andrologia 50 (2018), https://doi.org/10.1111/and.12871.
[38] R. Jakhar, K. Crasta, Exosomes as emerging pro-tumorigenic mediators of the senescence-associated secretory phenotype, Int J. Mol. Sci. 20 (2019), https://doi.org/10.3390/ijms20102547.
[39] C. Théry, S. Amigorena, G. Raposo, et al., Isolation and characterization of exosomes from cell culture supernatants and biological fluids, Curr. Protoc. Cell Biol. Chapter 3 Unit 3 (2006) 22, https://doi.org/10.1002/0471143030.cb0322s30.
[40] M. Eldh, K. Ekström, H. Valadi, et al., Exosomes communicate protective messages during oxidative stress; possible role of exosomal shuttle RNA, PLoS One 5 (2010), e15353, https://doi.org/10.1371/journal.pone.0015353.
[41] F.J. Vizoso, N. Eiro, S. Cid, et al., Mesenchymal stem cell secretome: toward cell-free therapeutic strategies in regenerative medicine, Int J. Mol. Sci. 18 (2017), https://doi.org/10.3390/ijms18091852.
[42] C. Ide, Y. Nakai, N. Nakano, et al., Bone marrow stromal cell transplantation for treatment of sub-acute spinal cord injury in the rat, Brain Res 1332 (2010) 32–47, https://doi.org/10.1016/j.brainres.2010.03.043.
[43] I. Chimenti, R.R. Smith, T.S. Li, et al., Relative roles of direct regeneration versus paracrine effects of human cardiosphere-derived cells transplanted into infarcted mice, Circ. Res. 106 (2010) 971–980, https://doi.org/10.1161/circresaha.109.210682.
[44] C. Toma, M.F. Pittenger, K.S. Cahill, et al., Human mesenchymal stem cells differentiate to a cardiomyocyte phenotype in the adult murine heart, Circulation 105 (2002) 93–98, https://doi.org/10.1161/hc0102.101442.
[45] G. Maguire, Stem cell therapy without the cells, Commun. Integr. Biol. 6 (2013), e26631, https://doi.org/10.4161/cib.26631.
[46] A. Bonauer, R.A. Boon, S. Dimmeler, Vascular microRNAs, Curr. Drug Targets 11 (2010) 943–949, https://doi.org/10.2174/138945010791591313.
[47] E. Gascon, F.B. Gao, Cause or effect: misregulation of microrna pathways in neurodegeneration, Front Neurosci. 6 (2012) 48, https://doi.org/10.3389/fnins.2012.00048.
[48] R. Rupaimoole, F.J. Slack, MicroRNA therapeutics: towards a new era for the management of cancer and other diseases, Nat. Rev. Drug Discov. 16 (2017) 203–222, https://doi.org/10.1038/nrd.2016.246.
[49] X. Cao, Q. Ma, B. Wang, et al., Circ-E2F3 promotes cervical cancer progression by inhibiting microRNA-296-5p and increasing STAT3 nuclear translocation, Ann. N. Y Acad. Sci. 1507 (2022) 84–98, https://doi.org/10.1111/nyas.14653.
[50] H.K. Badawy, D.M. Abo-Elmatty, N.M. Mesbah, Differential expression of MicroRNA let-7e and 296-5p in plasma of Egyptian patients with essential hypertension, Heliyon 4 (2018), e00969, https://doi.org/10.1016/j.heliyon.2018.e00969.
[51] Q. Hu, G. Che, Y. Yang, et al., Histone deacetylase 3 aggravates type 1 diabetes mellitus by inhibiting lymphocyte apoptosis through the microRNA-296-5p/Bcl-xl axis, Front Genet. 11 (2020), 536854, https://doi.org/10.3389/fgene.2020.536854.
[52] X. Xu, Y. Dong, N. Ma, et al., MiR-337-3p lowers serum LDL-C level through targeting PCSK9 in hyperlipidemic mice, Metabolism 119 (2021), 154768, https://doi.org/10.1016/j.metabol.2021.154768.
[53] Z. Huang, N. Zhang, W. Ma, et al., MiR-337-3p promotes chondrocytes proliferation and inhibits apoptosis by regulating PTEN/AKT axis in osteoarthritis, Biomed. Pharm. 95 (2017) 1194–1200, https://doi.org/10.1016/j.biopha.2017.09.016.
[54] L.R. Bollu, A. Mazumdar, M.I. Savage, et al., Molecular pathways: targeting protein tyrosine phosphatases in cancer, Clin. Cancer Res 23 (2017) 2136–2142, https://doi.org/10.1158/1078-0432.Ccr-16-0934.
[55] W.J. Li, K. Park, J.S. Paick, et al., Chronic treatment with an oral rho-kinase inhibitor restores erectile function by suppressing corporal apoptosis in diabetic rats, J. Sex. Med. 8 (2011) 400–410, https://doi.org/10.1111/j.1743-6109.2010.01724.x.
[56] J. Wen, A. Grenz, Y. Zhang, et al., A2B adenosine receptor contributes to penile erection via PI3K/AKT signaling cascade-mediated eNOS activation, Faseb J. 25 (2011) 2823–2830, https://doi.org/10.1096/fj.11-181057.
[57] H. Lin, T. Wang, Y. Ruan, et al., Rapamycin supplementation may ameliorate erectile function in rats with streptozotocin-induced type 1 diabetes by inducing autophagy and inhibiting apoptosis, endothelial dysfunction, and corporal fibrosis, J. Sex. Med. 15 (2018) 1246–1259, https://doi.org/10.1016/j.jsxm.2018.07.013.
[58] X. Chen, Q. Yang, T. Zheng, et al., Neurotrophic effect of adipose tissue-derived stem cells on erectile function recovery by pigment epithelium-derived factor secretion in a rat model of cavernous nerve injury, Stem Cells Int. 2016 (2016) 5161248, https://doi.org/10.1155/2016/5161248.
[59] J. Park, H. Son, J.S. Chai, et al., Chronic administration of LIMK2 inhibitors alleviates cavernosal veno-occlusive dysfunction through suppression of cavernosal fibrosis in a rat model of erectile dysfunction after cavernosal nerve injury, PLoS One 14 (2019), e0213586, https://doi.org/10.1371/journal.pone.0213586.
[60] E. Wespes, Smooth muscle pathology and erectile dysfunction, Int. J. Impot Res. 14 (Suppl 1) (2002) S17–S21, https://doi.org/10.1038/sj.ijir.3900792.
[61] C. Macit, U.V. Ustundag, O.C. Dagdeviren, et al., The effects of calorie restriction and exercise on age-related alterations in corpus cavernosum, Front Physiol. 11 (2020) 45, https://doi.org/10.3389/fphys.2020.00045.
[62] D. Hu, Y. Ge, Y. Cui, et al., Upregulated IGFBP3 with Aging Is Involved in Modulating Apoptosis, Oxidative Stress, and Fibrosis: A Target of Age-Related Erectile Dysfunction, Oxid. Med. Cell Longev. 2022 (2022) 6831779, https://doi.org/10.1155/2022/6831779.
[63] X. Ouyang, X. Han, Z. Chen, et al., MSC-derived exosomes ameliorate erectile dysfunction by alleviation of corpus cavernosum smooth muscle apoptosis in a rat model of cavernous nerve injury, Stem Cell Res. Ther. 9 (2018) 246, https://doi.org/10.1186/s13287-018-1003-1.